



Published in final edited form as:

J Control Release. 2015 November 28; 218: 22–28. doi:10.1016/j.jconrel.2015.09.050.

Chemically Modified RNA Activated Matrices Enhance Bone Regeneration

Satheesh Elangovan^{1,*,#}, Behnoush Khorsand^{2,#}, Anh-Vu Do², Liu Hong³, Alexander Dewerth⁴, Michael Kormann⁴, Ryan D. Ross⁵, D. Rick Sumner⁵, Chantal Allamargot⁶, and Aliasger K. Salem^{1,2,*}

¹Department of Periodontics, University of Iowa College of Dentistry, Iowa City, IA

²Division of Pharmaceutics and Translational Therapeutics, University of Iowa College of Pharmacy, Iowa City, IA

³Department of Prosthodontics University of Iowa College of Dentistry, Iowa City, IA

⁴Department of Translational Genomics and Gene Therapy, University of Tübingen, Wilhelmstr. 56, Tübingen - 72074, Germany

⁵Department of Anatomy and Cell Biology, Rush Medical College, Chicago, IL

⁶Central Microscopy Research Facility, University of Iowa, Iowa City, IA

Abstract

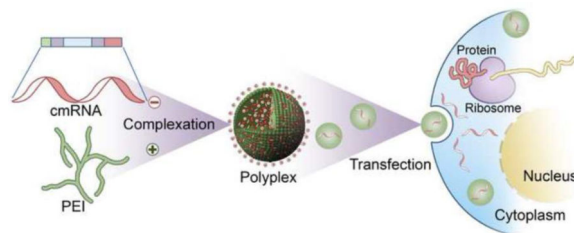
There exists a dire need for improved therapeutics to achieve predictable bone regeneration. Gene therapy using non-viral vectors that are safe and efficient at transfecting target cells is a promising approach to overcoming the drawbacks of protein delivery of growth factors. Here, we investigated the transfection efficiency, cytotoxicity, osteogenic potential and *in vivo* bone regenerative capacity of chemically modified ribonucleic acid (cmRNA) (encoding BMP-2) complexed with polyethylenimine (PEI) and made comparisons with PEI complexed with conventional plasmid DNA (encoding BMP-2). The polyplexes were fabricated at an amine (N) to phosphate (P) ratio of 10 and characterized for transfection efficiency using human bone marrow stromal cells (BMSCs). The osteogenic potential of BMSCs treated with these polyplexes was validated by determining the expression of bone-specific genes, *osteocalcin* and *alkaline phosphatase* as well as through the detection of bone matrix deposition. Using a calvarial bone defect model in rats it was shown that PEI-cmRNA (encoding BMP-2)-activated matrices promoted significantly enhanced bone regeneration compared to PEI-plasmid DNA (BMP-2)-activated matrices. Our proof of concept study suggests that scaffolds loaded with non-viral vectors harboring cmRNA encoding osteogenic proteins may be a powerful tool for stimulating bone regeneration with significant potential for clinical translation.

*To whom correspondence should be addressed: aliasger-salem@uiowa.edu or satheesh-elangovan@uiowa.edu.

#Joint first author

Publisher's Disclaimer: This is a PDF file of an unedited manuscript that has been accepted for publication. As a service to our customers we are providing this early version of the manuscript. The manuscript will undergo copyediting, typesetting, and review of the resulting proof before it is published in its final citable form. Please note that during the production process errors may be discovered which could affect the content, and all legal disclaimers that apply to the journal pertain.

Graphical abstract



Keywords

Chemically modified RNA; Plasmid DNA; Polyethylenimine; Gene delivery; bone morphogenetic protein-2; Bone regeneration

1. Introduction

The significant need for improved therapeutics promoting fracture healing and bone regeneration has led to the introduction and rapid expansion of biomimetic materials in medicine and dentistry [1–8]. One such advancement is the introduction of growth factors or morphogens, such as bone morphogenetic protein-2 (BMP-2) [9–13]. BMP-2 delivered as a human recombinant protein on an absorbable collagen sponge (INFUSE® Bone Graft, Medtronic Spinal and Biologics, Memphis, TN) was shown to be effective in the treatment of patients with degenerative disc disease, bone fractures, as well as oral and maxillofacial osseous defects [14, 15]. However, there are a number of drawbacks to using recombinant BMP-2 for both approved and off-label indications [16, 17]. In spite of its efficacy, the high cost associated with recombinant protein therapy, as well as the supraphysiological dosage required to compensate for the short half-lives of these proteins *in vivo* [18], raises serious concerns and strongly underscore the need for alternative approaches. One promising alternative is gene therapy based therapeutics. Gene therapies performed using viral vectors have demonstrated successful delivery of single or multiple transgenes for effective bone regeneration [19, 20]. Non-viral gene delivery vectors are relatively safe compared to viral vectors but have lower transfection efficiencies [21, 22]. The safety concerns and low transfection efficiencies associated with viral and non-viral gene therapies, respectively, are potential barriers for their clinical translation. Therefore, there is a great demand in both medicine and dentistry to develop novel regenerative strategies that are safe, cost-effective and that could potentially overcome the barriers associated with current protein and DNA based approaches.

Here we propose a novel delivery system with the potential to overcome most of the barriers of protein as well as DNA based therapeutics. Employing inexpensive yet safe biomaterials to embed and release [23] chemically modified ribonucleic acid (cmRNA) in a controlled manner addresses the high cost and safety concerns that exist with recombinant protein and viral based gene therapeutic approaches. By eliminating the need for nuclear trafficking [24] (the ultimate barrier for successful transfection in non-dividing cells), cmRNA delivery would potentially address the lower transfection efficiencies associated with non-viral gene

delivery systems [25, 26] and, since this strategy employs non-viral vectors, it alleviates the immunogenic concern that exists with viral vectors as well [27]. Other advantages include a simpler purification process and greater safety, as mRNA does not integrate into the genome [28]. Furthermore, the *in vivo* approach rather than *ex vivo* transfection will further reduce the treatment cost significantly [29]. Previous murine studies demonstrated the safety and efficacy of cmRNA-based therapeutics to treat lethal lung disease or to prevent allergic asthma *in vivo* [27]. The major limitation of using mRNA is the associated immunogenicity, mediated primarily through toll-like receptors (TLR)- 3, 7 and 8 [30, 31]. However, modifying the nucleotides significantly contributed to a reduction in immunogenicity whilst retaining its function [32]. ***To the best of our knowledge, this is the first study demonstrating the tissue regenerative potential of cmRNA-based therapeutics.*** Specifically, synthesized and well-characterized polyplexes of cmRNA and polyethylenimine (PEI) were embedded into collagen matrices which, upon implantation into rat calvarial defects, resulted in enhanced bone regeneration.

2. Materials and methods

2.1. Materials

Branched PEI (mol. wt. 25 kDa), the GenElute™ HP endotoxin-free plasmid maxiprep kit and sodium thiosulfate were obtained from Sigma-Aldrich® (St. Louis, MO). The BMP-2 ELISA kit was purchased from Quantikine® (R & D Systems®, Minneapolis, MN). Plasmid DNA (6.9 Kb) encoding BMP-2 protein driven by cytomegalovirus promoter/enhancer was obtained from Origene Technologies, Inc. (Rockville, MD). The RNA-easy kit was purchased from Qiagen Inc. The TaqMan Reverse Transcription Reagents and 18S-rRNA were purchased from Applied Biosystems (Foster City, CA). Absorbable type-I bovine collagen was obtained from Zimmer Dental Inc. (Carlsbad, CA). Human bone marrow stromal cells (BMSCs) were purchased from American Type Culture Collection (ATCC®, Manassas, VA). Dulbecco's modified eagle medium (DMEM), trypsin-EDTA (0.25%, 1X solution) and Dulbecco's phosphate buffered saline (PBS) were purchased from Gibco® (Invitrogen™, Grand Island, NY). Fetal bovine serum (FBS) was obtained from Atlanta Biologicals® (Lawrenceville, GA). Gentamycin sulfate (50 mg/ml) was purchased from Mediatech Inc. (Manassas, VA). All other chemicals and solvents used were of reagent grade.

2.2. Preparation of cmRNA encoding BMP-2

To generate templates for *in vitro* transcription, BMP-2 cDNA was cut out of its original vector and subcloned into a PolyA-120 containing T7 pVAX1 (Life Technologies, Madison, WI). Plasmids were linearized with XbaI, following which, its purity was verified and quantified spectrophotometrically. Using MEGAscript T7 Transcription Kits (Life Technologies, Madison, WI) mRNA of BMP-2 was synthesized and capped with the anti-reverse cap analog (*ARCA*; 7-methyl (3'-O-methyl) GpppGm7G (5')ppp(5')G). To achieve mRNA modification, the following modified ribonucleic acid triphosphates were added to the reaction at a ratio of 25%: 2-thiouridine-5'-triphosphate and 5-methylcytidine-5'-triphosphate (*s2U(0.25)m5C(0.25)*) as well as pseudouridine-5'-triphosphate and 5-methylcytidine-5'-triphosphate (*Ψ(1.0)m5C(1.0)*) at a ratio of 100%. Synthesized mRNA

was purified and analyzed for size and purity. Once the cmRNA of BMP-2 was synthesized, the degree of immune response to cmRNA was evaluated. Unmodified mRNA and cmRNA of BMP-2 were injected into the peritoneum of BALB/c mice and serum levels of IFN- α (R&D systems, Minneapolis, MN) were measured by ELISA, 24 hours post-injection.

2.3. Preparation of pDNA encoding BMP-2

The chemically competent DH5 α TM bacterial strain (*Escherichia coli* species) was transformed with *pDNA* to amplify the plasmid. The *pDNA* in the transformed cultures was then expanded in *E. coli* in Lennox L Broth (LB Broth) overnight at 37°C in an incubator shaker at 300 rpm. Plasmid DNA was extracted using GenEluteTM HP endotoxin-free plasmid maxiprep kit and was analyzed for purity using a NanoDrop 2000 UV-Vis Spectrophotometer (Thermoscientific, Wilmington, DE) by measuring the ratio of absorbance (A_{260}/A_{280} nm). The concentration of *pDNA* solution was determined by absorbance at 260 nm.

2.4. Fabrication of PEI-pDNA and PEI-cmRNA polyplexes

PEI-*pDNA* polyplexes were prepared by adding 50 μ L PEI solution to 50 μ L *pDNA* (BMP-2) solution containing 25 μ g *pDNA* and mixed by vortexing for 30 s. The mixture was incubated at room temperature for 30 min to allow complex formation between the positively charged PEI (amine groups) and the negatively charged *pDNA* (phosphate groups). To achieve optimal transfection efficacies, polyplexes were fabricated using N (nitrogen) to P (phosphate) ratios (molar ratio of amine groups of PEI to phosphate groups in *pDNA* backbone) of 10 [22]. Similarly, PEI-cmRNA polyplexes at N/P of 10 were synthesized by mixing 50 μ L of PEI solution to 50 μ L cmRNA encoding BMP-2 containing various amounts of cmRNA for 30 s. For *in vitro* transfection experiments, we utilized PEI-cmRNA polyplexes containing final amounts of 0.2, 0.72 or 1.2 μ g of cmRNA (BMP-2). For *in vivo* testing we prepared polyplexes containing final amounts of 25 μ g of cmRNA (BMP-2) that was then added to the collagen scaffolds, prior to implantation.

2.5. In vitro evaluation of cytotoxicity of PEI-pDNA and PEI-cmRNA polyplexes at a N/P ratio of 10 in BMSCs

Cytotoxicity of PEI-pDNA and PEI-cmRNA polyplexes on BMSCs, at an N/P ratio of 10 was evaluated using an MTS cell growth assay (Cell Titer 96 AQueous One Solution cell proliferation assay, Promega Corporation). Cells were seeded at a density of 10,000 cells/well in clear polystyrene, flat bottomed, 96-well tissue culture grade plates (Costar®, Corning Inc.) and allowed to attach overnight. The next day, at a cell confluence ~80%, the cell culture medium was changed to serum-free medium and the treatments were gently mixed and added drop-wise into the wells. Each well was treated with 20 μ L of polyplexes containing 1 μ g of *pDNA* or cmRNA. Untreated BMSCs were used as controls. Cells treated with PEI alone served as additional controls. To mimic the conditions used in the transfection experiments, the polyplexes were incubated with the cells for 4 h. At the end of the incubation period, the cells were washed with 1X PBS and fresh complete medium was added. After a total incubation time of 48 h, cells were washed with 1X PBS and fresh complete medium was added to the cells followed by addition of 20 μ L MTS (3-(4,5-

dimethylthiazol-2-yl)-5-(3-carboxymethoxyphenyl)-2-(4-sulfophenyl)-2H-tetrazolium) cell growth assay reagent. The plates were then incubated at 37°C in a humidified 5% CO₂ atmosphere for 3 h. The amount of soluble formazan produced by reduction of MTS reagent by viable cells was measured spectrophotometrically using SpectraMax® Plus384 (Molecular Devices, Sunnyvale, CA) at 490 nm. The cell viability was expressed by the following equation: cell viability (%) = (absorbance intensity of treated cells/absorbance intensity of untreated cells (control)) × 100. Values are expressed as mean ± SD and each treatment was performed in quadruplicate.

2.6. In vitro evaluation of transfection of BMSCs with PEI-pDNA and PEI-cmRNA polyplexes

The bone marrow stromal cells (BMSCs) were plated in 24-well plates at a seeding density of 8×10^4 cells/well 24 h prior to treatments. BMSCs were treated with the PEI-*pDNA* polyplexes containing 1 µg *pDNA* and the PEI-cmRNA polyplexes containing 0.2, 0.75 and 1.20 µg of cmRNA encoding BMP-2 all synthesized at a N/P of 10 for 4 h at 37°C and then followed by a subsequent wash with PBS (1X). After a total incubation time of 48 h, BMSCs were treated with heparin (10 mg/mL) for 4 h to prevent BMP-2 protein retention on the BMSC surface. The cell culture supernatants were assayed for BMP-2 protein levels using an ELISA kit. Untreated cells were employed as controls. The mean value was recorded as the average of four measurements.

2.7. Real-time PCR (RT-PCR) analysis

Osteoblast genotypic markers tested were osteocalcin and alkaline phosphatase. On day 3 post-transfection, total RNA was extracted from BMSCs using RNeasy kit (Qiagen Inc, Valencia, CA). RNA extracts were normalized for PCR analysis using a spectrophotometer at 260 nm. Complementary DNA (cDNA) was generated by reverse transcription of the normalized RNA and was amplified using TaqMan Reverse Transcription Reagents. cDNA samples (3 µL for a total volume of 75 µL per reaction) were analyzed both for targeted osteogenic genes, as well as 18S-rRNA as a control (Undisclosed sequences, Applied Biosystems, Foster City, CA). Real-time PCR reactions were performed in 96-well Optical Reaction Plates (Applied Biosystems, Foster City, CA), using a 7300 real-time PCR system (Applied Biosystems, Foster City, CA).

2.8. Von-Kossa staining

The osteogenic differentiation of BMSCs was studied after 14 days of receiving the various treatments using Von-Kossa staining. The cell cultures were washed with PBS (1X) and fixed in 4% paraformaldehyde (Alfa Aesar, Ward Hill, MA) for 30 min. Then cells were washed with water, and a 5% silver nitrate solution (Fisher Scientific, Pittsburgh, PA) was added and the plate was exposed to UV for 40 min, after which the plate was rinsed with water several times. Sodium thiosulfate (5%) (Sigma-Aldrich) was added for 5 min and then the plate was rinsed in water and 1% Nuclear Fast Red solution (Rowley Biochemical Institute, Danvers, MA) was added for 5 min. The plate was washed with water, followed by dehydration with ethanol, and dried for imaging. The cells were imaged with the Nikon TE-300 inverted microscope.

2.9. Alizarin red staining

In addition to Von-Kossa staining, the calcium deposition by BMSCs was assessed using Alizarin red staining. After 14 days, the cell cultures were washed with PBS (1X) for 5 min and fixed in 10% formalin (Alfa Aesar, Ward Hill, MA) for 10 min. Then cells were washed with water, and 2% Alizarin red S at a pH range of 4.1 – 4.3 (Sigma-Aldrich,) was added to the wells for 10 min. Then the plate was rinsed with distilled water several times until no additional Alizarin red continued to seep into the solution, and was then dried for imaging. The cells were imaged with the Nikon TE-300 inverted microscope.

2.10. Atomic absorption spectroscopy

Released Ca^{2+} ions from BMSCs were measured with a flame atomic absorption spectrophotometer (Perkin Elmer Model 2380). Cells were acid hydrolyzed 14 days post transfection using 0.6 N HCL overnight. Samples were prepared by combining 450 μL of acid hydrolyzed samples with 550 μL of 2.5% La_2O_3 in 0.6 N HCl. The samples were measured at 422.7 nm with a Perkin Elmer intenistron calcium lamp, a slit of 0.7 nm, and energy of 49 keV. The instrument was calibrated using commercial calcium standards. Calcium standards were prepared by dissolving 20 ppm calcium stock in required volumes of solution containing 0.6 N HCl in 1X PBS and 2.5 % lanthanum oxide.

2.11. In vivo implantation of complex embedded collagen scaffolds

Fisher (CDF®) male white rats (F344/ DuCrI, 14 weeks old, 250 g) were purchased from Harlan Laboratories (Indianapolis, IN) and housed and cared for in the animal facilities. All animal protocols used in these studies were approved by and performed according to guidelines established by the University of Iowa Institutional Animal Care and Use Committee, Iowa. The animals were anaesthetized by intra-peritoneal injection of the mixture of ketamine (80 mg/kg) and xylazine (8 mg/kg). Following a sagittal incision in the scalp, the soft tissues were reflected using blunt dissection to expose the calvarium. Using a round carbide bur, two critical-sized defects (5 mm diameter \times 2 mm thickness) were generated on the parietal bone, on both sides of the sagittal suture. The four groups employed in this study were: 1) empty defect (n=7); 2) defect implanted with PEI loaded collagen scaffold (n=7); 3) defect treated with PEI-*pDNA* complex-loaded collagen scaffold (n=7); and 4) defect treated with PEI-cmRNA complex-loaded collagen scaffold (n=7). Where applicable, the scaffold was cut into cylinders with a diameter of 5 mm and a thickness of 2 mm and the solution, containing PEI complexes, was injected into each scaffold which was then implanted into the rats. Next, using sterile silk sutures the incision was closed and buprenorphine (0.15 mg), was administered intramuscularly for pain management. Rats were euthanized after 4 weeks, the regions of interest were cut from the calvarial bone, dissected and fixed in neutral buffered formalin (10%) for analyses.

2.12. Micro-computed tomography (μCT) analysis

To quantitatively measure the amount of bone formed, three-dimensional x-ray micro-computed tomography (μCT) imaging was performed. A cone-beam μCT system (μCT 40, Scanco Medical AG, Switzerland) was utilized to scan the specimens in 70% ethanol at a source voltage of 55 kVp and beam current of 145 μA with a voxel size of 10 μm and an

integration time of 300 ms. The region of interest analyzed consisted of a constant 3.5 mm diameter circular region that was placed in the center of the machined defect and spanned a total of 50 reconstructed slices. Using the manufacturer's software (sigma = 0.8, support = 1.0, and threshold = 250) approximately 3.8 mm³ (oriented perpendicular to the outer table of the calvarium) of each defect in the specimen was analyzed. Bone volume (BV) per total volume (TV) and connectivity density parameters were calculated using the μ CT software.

2.13. Histological observation of rat bone samples

After completing the μ CT, the specimens (empty defect, PEI-*pDNA* complex-loaded scaffolds, and PEI-cmRNA complex-loaded scaffolds) were decalcified using a Surgipath Decalcifier II procedure. The specimens were embedded in paraffin after dehydration in ascending concentrations of ethanol, followed by treatment with xylene (Merck, Germany). Histological sections (5 μ m) in the central portion of the wound were prepared in the sagittal plane and collected on Superfrost Plus Slides (Fisher Scientific, Pittsburgh, PA). Sections were deparaffinized and stained with Hematoxylin-Eosin (H & E staining) according to standard protocols. To evaluate *in vivo* bone regeneration after 4 weeks; six sections, representing the central area of each defect, including intact native bone margins surrounding the reconstructed defects, were used to assess new bone formation and bridging of the created defect. The Olympus Stereoscope SZX12 and an Olympus BX61 microscope, both equipped with a digital camera, were utilized for the bright field examination of the slides.

2.14. Statistical analysis

Numerical data are represented as mean (\pm SD). All statistical analyses were performed using statistical and graphing software, GraphPad Prism version 5.02 for windows (GraphPad Software Inc., San Diego, CA). Unless otherwise stated the following stats were used; treatment groups were compared using Kruskal–Wallis and one-way analysis of variance followed by Dunnett's post-test analysis comparing all pairs of treatments. Differences were considered significant at p-values that were less than or equal to 0.05.

3. Results and discussion

This report investigates the safety and efficacy of cmRNA activated matrix in bone regeneration in rats. This form of RNA activated matrix provides localized transient protein therapy, since the nuclear translocation (the rate limiting step in gene therapy) is not required with this strategy. For the first time, we synthesized and thoroughly characterized cmRNA (BMP-2) alone, the PEI-cmRNA (BMP-2) polyplexes alone and also after embedding them in the collagen scaffold. Using appropriate controls, we further demonstrated the *in vivo* bone regeneration capacity of this novel RNA activated matrix in rat calvarial bone defect (CBD).

3.1. Generation of cmRNA and pDNA encoding BMP-2 proteins

Two chemically modified versions of BMP-2-encoding mRNA were transcribed (fig 1a). One version involved the substitution of 25% of uridine and cytidine in the mRNA sequence with 2-thiouridine-5' -triphosphate and 5-methylcytidine-5' -triphosphate

(s2U(0.25)m5C(0.25)), respectively, whilst the other version involved the substitution of 100% of uridine and cytidine with pseudouridine-5'-triphosphate and 5-methylcytidine-5'-triphosphate ($\Psi(1.0)m5C(1.0)$), respectively. Initially, both modified mRNA sequences were compared with the unmodified mRNA for their ability to induce an innate immune inflammatory response as defined by the production of interferon- α (IFN- α) in mice. As desired, the mRNA modified using $\Psi(1.0)m5C(1.0)$ substitutions did not induce IFN- α production [27, 32], and was therefore used in subsequent experiments (fig 1b).

3.2. Morphology, size and surface charge of PEI-cmRNA polyplexes

The cmRNA prepared above was then complexed with PEI through electrostatic condensation. The PEI-cmRNA polyplexes size, charge, and morphology at a N/P ratio of 10 were assessed using a Zetasizer Nano-ZS and transmission electron microscopy (TEM). The polyplexes were 153 nm (\pm 2 nm) in diameter with a net surface charge of +37.7 mV (fig 2). The polyplexes had narrow size distributions with the average polydispersity index (PDI) equal to 0.1. The inset of figure 2 shows a TEM image of the polyplexes, demonstrating spherical polyplexes with monomodal distribution. The small size as well as the positive surface charge of the polyplexes are both critical for efficient *in vitro* cellular uptake by clathrin-mediated endocytosis [34] as well as *in vivo* distribution and diffusion [35] in the target tissues.

3.3. In vitro cell viability assay for PEI-pDNA and PEI-cmRNA polyplexes

The cytotoxicity of polyplexes, containing 1 μ g of *pDNA* or cmRNA, at a N/P ratio of 10 was evaluated over 48 h using a MTS assay. Figure 3 demonstrates that BMSCs viabilities were approximately 75% and 85% when transfected with PEI-*pDNA* and PEI-cmRNA polyplexes, respectively. Although the trend toward greater viabilities for BMSCs treated with PEI-cmRNA versus PEI-*pDNA* was not statistically significant, it was, however, noted that the decrease in cell viability for BMSCs treated with PEI-*pDNA* compared to untreated BMSCs was statistically significant (** $p < 0.001$). The difference in cell viabilities between untreated BMSCs and PEI-cmRNA treated BMSCs was not significant. These data suggest that PEI-cmRNA polyplexes may have an advantage over PEI-*pDNA* polyplexes in terms of maintaining higher cell viabilities.

3.4. In vitro investigation of gene expression by PEI-pDNA and PEI-cmRNA polyplexes

The ability of the synthesized PEI-*pDNA* and PEI-cmRNA polyplexes to transfect BMSCs was evaluated through expression of BMP-2. BMPs are potent morphogens that belong to the transforming growth factor beta (TGF- β) super family and are known for their ability to induce ectopic bone formation, maintain post-natal skeletal homeostasis and to play a role in bone regeneration [33]. BMP-2 is an osteogenic factor which initiates bone formation and healing [36] while inducing the expression of other BMPs [37]. As demonstrated in figure 4, BMSCs transfected with PEI-cmRNA polyplexes resulted in significantly higher levels of BMP-2 compared to cells treated with PEI-*pDNA* polyplexes (p value = 0.0011, Kruskal-Wallis test). After transfection of cells with PEI-cmRNA, BMP-2 was secreted into the cell culture supernatant at concentrations approximately 3 times higher than cells treated with the PEI-*pDNA*. Furthermore, in the BMSCs treated with PEI-cmRNA polyplexes dose-

titratable expression of BMP-2 was observed which is known as one of the modified-mRNA technology properties that make it a powerful platform for directing cell fate [38]. These results revealed superior transfection efficiency of the cmRNA complexed with PEI, compared to PEI-*pDNA* polyplexes.

3.5. In vitro evaluation of bone osteogenic differentiation of BMSCs pretreated by PEI-*pDNA* and PEIcmRNA polyplexes

The osteogenic potential of BMSCs treated with PEI-*pDNA* and PEI-cmRNA polyplexes was assessed using real time PCR to measure the levels of transcription of bone-specific genes, *osteocalcin* (OCN) and *alkaline phosphatase* (ALP). Cells were transfected with polyplexes prepared at an N/P ratio of 10 and containing 1.2 µg of *pDNA* (encoding BMP-2) or cmRNA (encoding BMP-2) for 4 h, followed by further incubation for 3 days. The expression levels of OCN in BMSCs that were pretreated with PEI-cmRNA was significantly higher than the levels detected in controls (P value = 0.0013, Dunnett's multiple comparison test). Similarly, ALP levels detected in BMSCs that had been pretreated with PEI-cmRNA were slightly higher, albeit not significantly, compared to the levels detected in controls (fig 5). The *in vitro* levels of bone-specific markers such as ALP and OCN in the differentiated BMSCs are associated with their *in vivo* bone regenerative capabilities [39], therefore the enhancement of ALP and OCN expression in cells treated with PEI-cmRNA suggests that these cells have higher bone regenerative potential.

3.6. In vitro evaluation of bone matrix deposition by Von-Kossa, Alizarin Red staining and atomic absorption spectroscopy

Extracellular matrix calcification was evaluated in the BMSCs transfected with PEI-*pDNA* and PEI-cmRNA polyplexes after 14 days using qualitative (Von-kossa and Alizarin red staining) and quantitative (atomic adsorption spectroscopy) methods. Qualitative assessment revealed that the cells that had been pretreated with PEI-cmRNA appeared to stain darker, or more intensely, than PEI-*pDNA* pretreated BMSCs (fig 6a and 6b).

Calcium deposition 14 days post transfection was quantitatively analyzed using an atomic absorption spectrophotometer. Cells transfected with PEI-cmRNA promoted significantly higher levels of calcium deposition compared to untreated cells as well as cells transfected with PEI-*pDNA* polyplexes (p value <0.0001, Tukey's multiple comparison post-test). In contrast, cells transfected with PEI-*pDNA* demonstrated only an increase in calcium content compared to the untreated cells that was not statistically significant (fig 6c). The results presented here indicate enhanced osteogenic differentiation as evidenced by increased calcium deposition in BMSCs transfected with PEI-cmRNA polyplexes compared to the cells transfected with PEI-*pDNA* and control.

3.7. In vivo bone regeneration

The functional potency of collagen scaffolds loaded with either PEI-*pDNA* polyplexes or PEI-cmRNA polyplexes was evaluated *in vivo* using a CBD model in rats. The *in vivo* efficacy of the following four treatment groups was evaluated: (1) empty defect, (2) defect implanted with collagen scaffold treated with PEI, (3) defect implanted with PEI-*pDNA* polyplexes entrapped in collagen scaffold, and (4) defect implanted with PEI-cmRNA

polyplexes entrapped in collagen scaffold. After 4 weeks of *in vivo* implantation of the collagen scaffolds, rats were sacrificed and newly-formed bone tissue was evaluated using Micro-computed tomography (μ CT) scans. The μ CT scans revealed increased quantities of mineralized bone matrix in the CBDs treated with collagen scaffolds containing PEI-cmRNA polyplexes, compared to other treatment groups (fig 7a). The amount of bone tissue regenerated was quantified by analyzing the mineralized bone volume as a fraction of the total tissue volume of interest (BV/TV) and connectivity density of the regenerated bone. The BV/TV was 3.94-fold and 1.94-fold higher in defects treated with PEI-cmRNA and PEI-*pDNA* complex-embedded scaffolds, respectively, when compared to the empty defect (control) group. The distribution of BV/TV of defects treated with PEI-cmRNA was significantly higher compared to empty defects ($p = 0.039$, Kruskal–Wallis test) (fig 7b). Compared to the empty defect control group, the connectivity density of the regenerated bone was 14.07-fold and 5.82-fold greater for the PEI-cmRNA and PEI-*pDNA* complex-embedded scaffolds, respectively. The difference between connectivity density of the PEI-cmRNA group and the empty defect group was significant ($p = 0.0028$, Kruskal–Wallis test) (fig 7c). Evaluation of bone regeneration using histological images further validated the μ CT results. For the PEI-cmRNA complex-embedded scaffolds, extensive bridging of the defect by the mature, mineralized bone tissue was observed, while the PEI-*pDNA* complex-embedded scaffolds promoted mostly soft tissue regeneration with only small amounts of new bone formation at the defect margins. In contrast, the untreated defects remained unfilled (fig 7d).

4. Conclusion

In this proof of concept study, the safety and efficacy of cmRNA based therapeutics in bone regeneration is demonstrated for the first time in rats. It's clear that cmRNA encoding BMP-2 (at equivalent dosage) surpassed its *pDNA* counterpart in both biocompatibility and bone regeneration capacity. As mentioned earlier, cmRNA therapeutics has significant potential to be translated to clinics in both orthopedics and in dentistry, where the need for cost-effective bone replacement grafts is enormous. Our study clearly underscores the promising translational potential of this novel therapeutic strategy for tissue engineering applications, particularly bone regeneration. Future studies will explore other non-viral vectors and scaffolds to enhance the uptake of polyplexes in target tissue, thereby enhancing tissue regeneration further.

Acknowledgments

This study was supported by NIH R21 grant (1R21DE024206-01A1), the University of Iowa Start-up Grant, the ITI Foundation for the Promotion of Implantology, Switzerland (ITI Research Grant No. 855 2012), the Osteology Foundation Grant (12-054), the Sunstar - American Academy of Periodontology Foundation Research Fellowship, and the Lyle and Sharon Bighley Professorship. Rush University Medical Center MicroCT/Histology Core resources were used. Imaging equipment at the University of Iowa Core Microscopy Research Facility was used. We acknowledge technical support from Katherine Walters and Denise Seabold.

References

1. Deschaseaux F, Pontikoglou C, Sensébé L. Bone regeneration: the stem/progenitor cells point of view. *J. Cell. Mol. Med.* 2010; 14:103–115. [PubMed: 19840188]

2. Jha AK, Mathur A, Svedlund FL, Ye JQ, Yeghiazarians Y, Healy KE. Molecular weight and concentration of heparin in hyaluronic acid-based matrices modulates growth factor retention kinetics and stem cell fate. *J Control Release*. 2015; 209:308–316. [PubMed: 25931306]
3. Wang Q, Li H, Xiao Y, Li S, Li B, Zhao XW, Ye L, Guo B, Chen XM, Ding Y, Bao CY. Locally controlled delivery of TNF alpha antibody from a novel glucose-sensitive scaffold enhances alveolar bone healing in diabetic conditions. *J Control Release*. 2015; 206:232–242. [PubMed: 25796348]
4. Kim SH, Kim SH, Jung Y. TGF-beta(3) encapsulated PLCL scaffold by a supercritical CO₂-HFIP co-solvent system for cartilage tissue engineering. *J Control Release*. 2015; 206:101–107. [PubMed: 25804870]
5. Vo TN, Ekenseair AK, Spicer PP, Watson BM, Tzouanas SN, Roh TT, Mikos AG. In vitro and in vivo evaluation of self-mineralization and biocompatibility of injectable, dual-gelling hydrogels for bone tissue engineering. *J Control Release*. 2015; 205:25–34. [PubMed: 25483428]
6. Quinlan E, Lopez-Noriega A, Thompson E, Kelly HM, Cryan SA, O'Brien FJ. Development of collagen-hydroxyapatite scaffolds incorporating PLGA and alginate microparticles for the controlled delivery of rhBMP-2 for bone tissue engineering. *J Control Release*. 2015; 198:71–79. [PubMed: 25481441]
7. Suliman S, Xing Z, Wu XJ, Xue Y, Pedersen TO, Sun Y, Doskeland AP, Nickel J, Waag TL, Lygre H, Finne-Wistrand A, Steinmuller-Nethl D, Krueger A, Mustafa K. Release and bioactivity of bone morphogenetic protein-2 are affected by scaffold binding techniques in vitro and in vivo. *J Control Release*. 2015; 197:148–157. [PubMed: 25445698]
8. Do AV, Khorsand B, Geary SM, Salem AK. 3D Printing of Scaffolds for Tissue Regeneration Applications. *Adv Healthc Mater*. 2015
9. Canalis E, McCarthy T, Centrella M. Growth factors and the regulation of bone remodeling. *The Journal of Clinical Investigation*. 1988; 81:277–281. [PubMed: 3276726]
10. Seo BB, Choi H, Koh JT, Song SC. Sustained BMP-2 delivery and injectable bone regeneration using thermosensitive polymeric nanoparticle hydrogel bearing dual interactions with BMP-2. *J Control Release*. 2015; 209:67–76. [PubMed: 25910579]
11. Quinlan E, Thompson EM, Matsiko A, O'Brien FJ, Loez-Noriega A. Long-term controlled delivery of rhBMP-2 from collagen-hydroxyapatite scaffolds for superior bone tissue regeneration. *J Control Release*. 2015; 207:112–119. [PubMed: 25817394]
12. Karfeld-Sulzer LS, Ghayor C, Siegenthaler B, de Wild M, Leroux JC, Weber FE. N-methyl pyrrolidone/bone morphogenetic protein-2 double delivery with in situ forming implants. *J Control Release*. 2015; 203:181–188. [PubMed: 25697800]
13. Atluri K, Seabold D, Hong L, Elangovan S, Salem AK. Nanoplex-Mediated Co-delivery of Fibroblast Growth Factor and Bone Morphogenetic Protein Genes Promotes Osteogenesis in Human Adipocyte-Derived Mesenchymal Stem Cells. *Mol Pharm*. 2015
14. Boyne PJ, Lilly LC, Marx RE, Moy PK, Nevins M, Spagnoli DB, Triplett RG. De Novo Bone Induction by Recombinant Human Bone Morphogenetic Protein-2 (rhBMP-2) in Maxillary Sinus Floor Augmentation. *J. Oral Maxillofac. Surg*. 2005; 63:1693–1707. [PubMed: 16297689]
15. Khan SN, Lane JM. The use of recombinant human bone morphogenetic protein-2 (rhBMP-2) in orthopaedic applications. *Expert Opin. Biol. Ther*. 2004; 4:741–748. [PubMed: 15155165]
16. Cancedda R, Giannoni P, Mastrogiacomo M. A tissue engineering approach to bone repair in large animal models and in clinical practice. *Biomaterials*. 2007; 28:4240–4250. [PubMed: 17644173]
17. Woo EJ. Adverse Events Reported After the Use of Recombinant Human Bone Morphogenetic Protein 2. *J. Oral Maxillofac. Surg*. 2012; 70:765–767. [PubMed: 22177811]
18. Tannoury CA, An HS. Complications with the use of bone morphogenetic protein 2 (BMP-2) in spine surgery. *Spine J*. 2014; 14:552–559. [PubMed: 24412416]
19. Evans CH. Gene therapy for bone healing. *Expert Rev. Mol. Med*. 2010; 12 null-null.
20. Evans CH, Ghivizzani SC, Robbins PD. Orthopedic gene therapy—lost in translation? *J. Cell. Physiol*. 2012; 227:416–420. [PubMed: 21948071]
21. Elangovan S, Karimbux N. Review Paper: DNA Delivery Strategies to Promote Periodontal Regeneration. *J. Biomater. Appl*. 2010; 25:3–18. [PubMed: 20511387]

22. Elangovan S, D'Mello SR, Hong L, Ross RD, Allamargot C, Dawson DV, Stanford CM, Johnson GK, Sumner DR, Salem AK. The enhancement of bone regeneration by gene activated matrix encoding for platelet derived growth factor. *Biomaterials*. 2014; 35:737–747. [PubMed: 24161167]
23. An YH, Woolf SK, Friedman RJ. Pre-clinical in vivo evaluation of orthopaedic bioabsorbable devices. *Biomaterials*. 2000; 21:2635–2652. [PubMed: 11071614]
24. Ponsaerts P, Van Tendeloo VFI, Berneman ZN. Cancer immunotherapy using RNA-loaded dendritic cells. *Clin. Exp. Immunol.* 2003; 134:378–384. [PubMed: 14632740]
25. Mockey M, Goncalves C, Dupuy FP, Lemoine FM, Pichon C, Midoux P. mRNA transfection of dendritic cells: synergistic effect of ARCA mRNA capping with Poly(A) chains in cis and in trans for a high protein expression level. *Biochem. Biophys. Res. Commun.* 2006; 340:1062–1068. [PubMed: 16403444]
26. Holtkamp S, Kreiter S, Selmi A, Simon P, Koslowski M, Huber C, Tureci O, Sahin U. Modification of antigen-encoding RNA increases stability, translational efficacy, and T-cell stimulatory capacity of dendritic cells. *Blood*. 2006; 108:4009–4017. [PubMed: 16940422]
27. Kormann MSD, Hasenpusch G, Aneja MK, Nica G, Flemmer AW, Herber-Jonat S, Huppmann M, Mays LE, Illenyi M, Schams A, Griese M, Bittmann I, Handgretinger R, Hartl D, Rosenecker J, Rudolph C. Expression of therapeutic proteins after delivery of chemically modified mRNA in mice. *Nat Biotech.* 2011; 29:154–157.
28. Yamamoto A, Kormann M, Rosenecker J, Rudolph C. Current prospects for mRNA gene delivery. *Eur. J. Pharm. Biopharm.* 2009; 71:484–489. [PubMed: 18948192]
29. Evans CH. Gene delivery to bone. *Advanced Drug Delivery Reviews*. 2012; 64:1331–1340. [PubMed: 22480730]
30. Ishii KJ, Akira S. TLR ignores methylated RNA? *Immunity*. 2005; 23:111–113. [PubMed: 16111629]
31. Kariko K, Ni H, Capodici J, Lamphier M, Weissman D. mRNA is an endogenous ligand for Toll-like receptor 3. *J. Biol. Chem.* 2004; 279:12542–12550. [PubMed: 14729660]
32. Karikó K, Buckstein M, Ni H, Weissman D. Suppression of RNA Recognition by Toll-like Receptors: The Impact of Nucleoside Modification and the Evolutionary Origin of RNA. *Immunity*. 2005; 23:165–175. [PubMed: 16111635]
33. Rosen V. BMP2 signaling in bone development and repair. *Cytokine Growth Factor Rev.* 2009; 20:475–480. [PubMed: 19892583]
34. Wagner E, Cotten M, Foisner R, Birnstiel ML. Transferrin-polycation-DNA complexes: the effect of polycations on the structure of the complex and DNA delivery to cells. *Proceedings of the National Academy of Sciences*. 1991; 88:4255–4259.
35. Ferkol T, Perales JC, Eckman E, Kaetzel CS, Hanson RW, Davis PB. Gene transfer into the airway epithelium of animals by targeting the polymeric immunoglobulin receptor. *The Journal of Clinical Investigation*. 1995; 95:493–502. [PubMed: 7860731]
36. Sakou T. Bone Morphogenetic Proteins: From Basic Studies to Clinical Approaches. *Bone*. 1998; 22:591–603. [PubMed: 9626397]
37. Sandberg MM, Aro HT, Vuorio EI. Gene expression during bone repair. *Clin. Orthop. Relat. Res.* 1993:292–312. [PubMed: 8472429]
38. Mandal PK, Rossi DJ. Reprogramming human fibroblasts to pluripotency using modified mRNA. *Nat. Protocols*. 2013; 8:568–582. [PubMed: 23429718]
39. Mauney JR, Jaquiéry C, Volloch V, Heberer M, Martin I, Kaplan DL. In vitro and in vivo evaluation of differentially demineralized cancellous bone scaffolds combined with human bone marrow stromal cells for tissue engineering. *Biomaterials*. 2005; 26:3173–3185. [PubMed: 15603812]

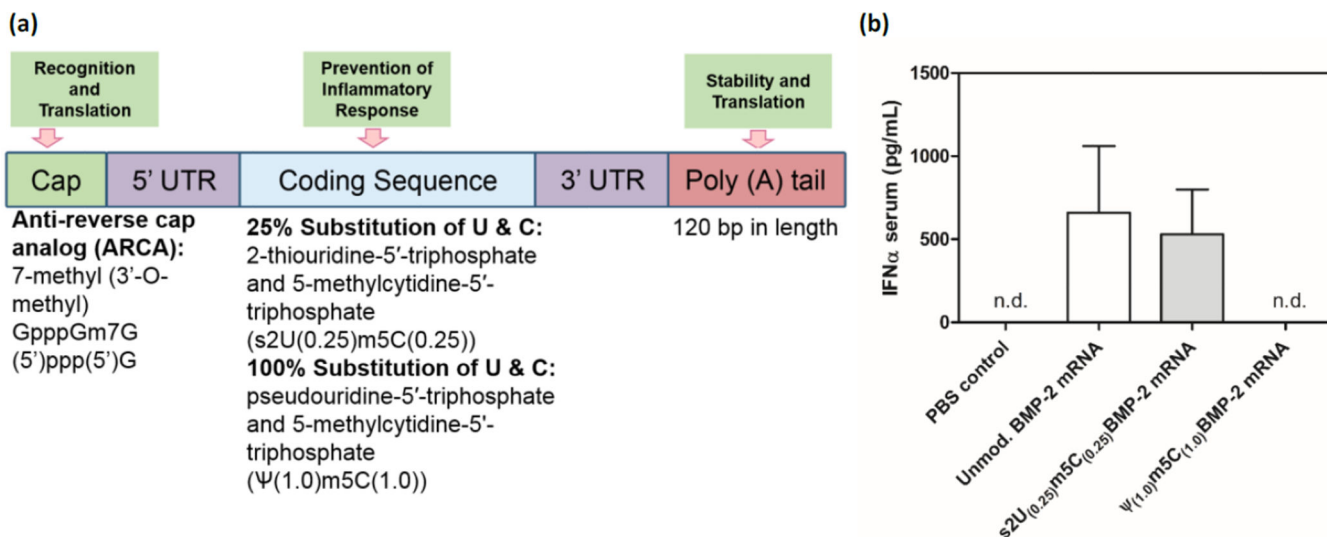


Fig. 1. (a) Scheme for modified mRNA construct with synthetic UTR and PolyA sequences attached to the coding sequence. (b) ELISA on sera to determine systemic IFN-α production 1 day following intra-peritoneal injections into BALB/c mice of 1 μg of cmRNA (s2U/m5C (25%), Ψ/m5C (100%)), or unmodified BMP-2 mRNA (n=3). Unmodified mRNA (BMP-2) and s2U/m5C (25%) induced high levels of IFN-α which was shown to be completely circumvented by Ψ/m5C (100%) modifications. n.d. non-detectable. Values are expressed as mean ± SD (n=3).

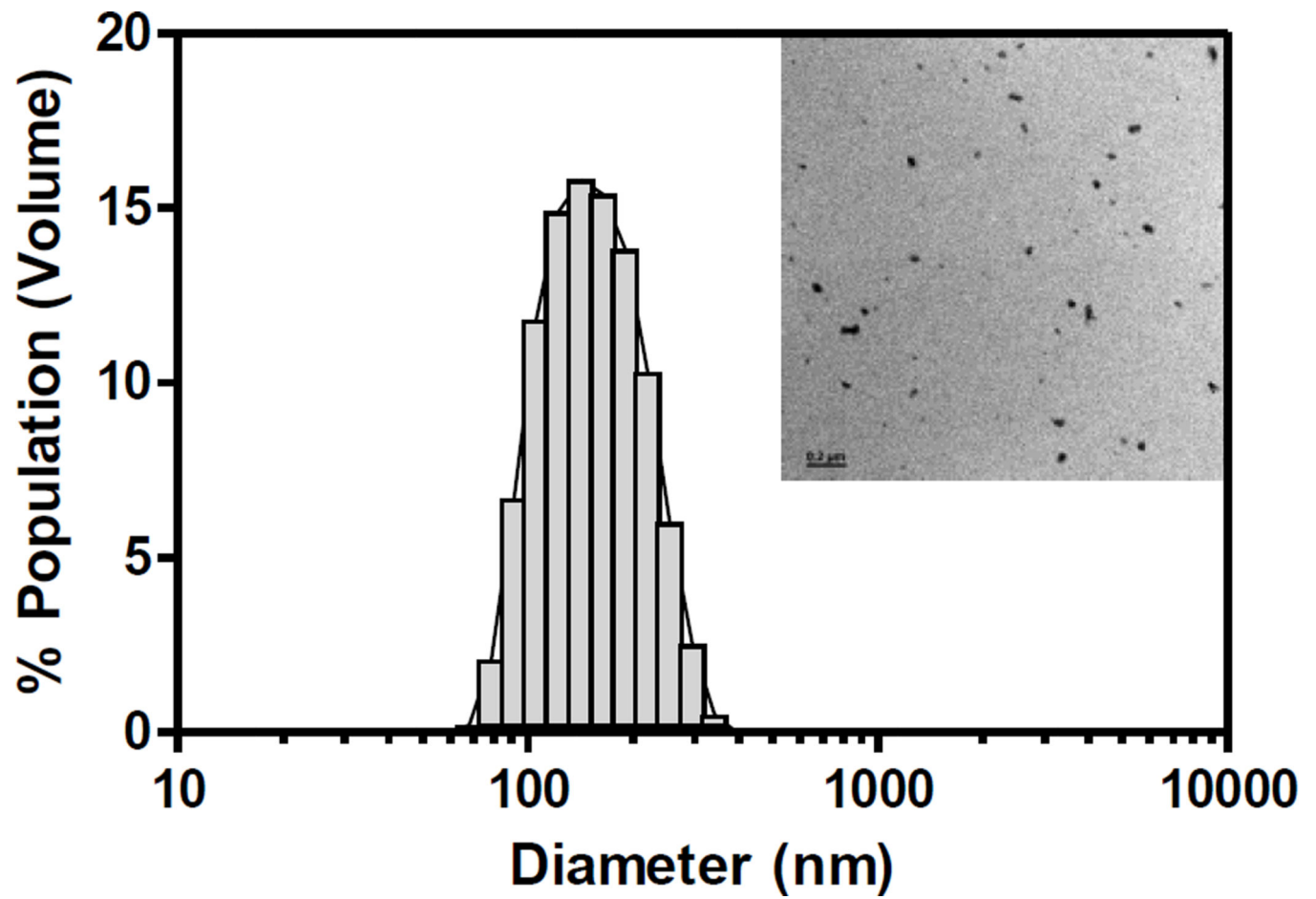


Fig. 2. Representative PEI-cmRNA polyplexes (N/P ratio 10) size distribution diagram as determined using Zetasizer Nano (inset: TEM image with scale bar = 0.2 μm)

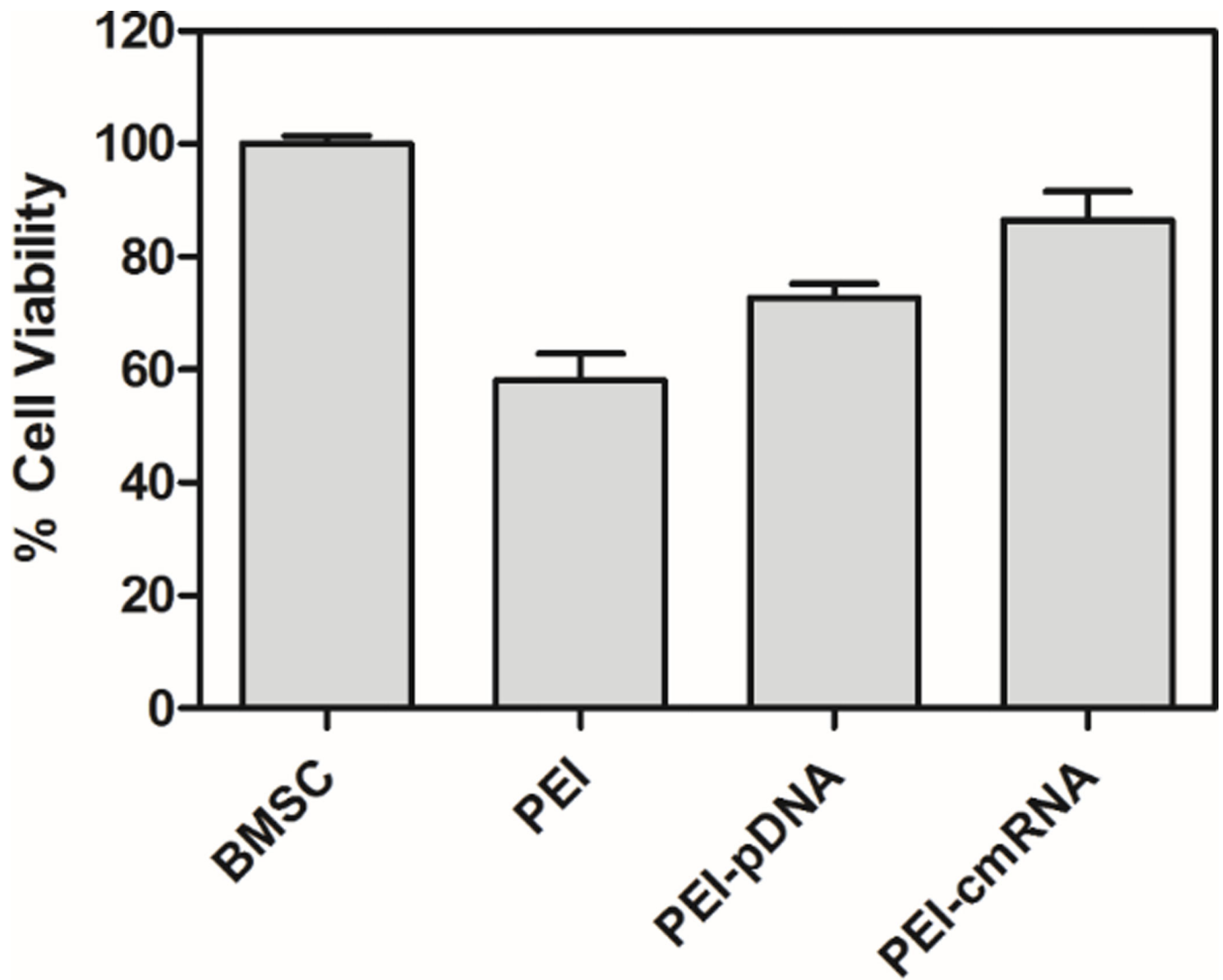


Fig. 3. MTS assay assessing the cytotoxicity of PEI-*pDNA* and PEI-cmRNA polyplexes in BMSCs after 48 h. Significant differences between the treatments and the untreated cells were assessed by one-way analysis of variance followed by Tukey's post-test (***p* < 0.001). Values are expressed as mean ± SD (n=4).

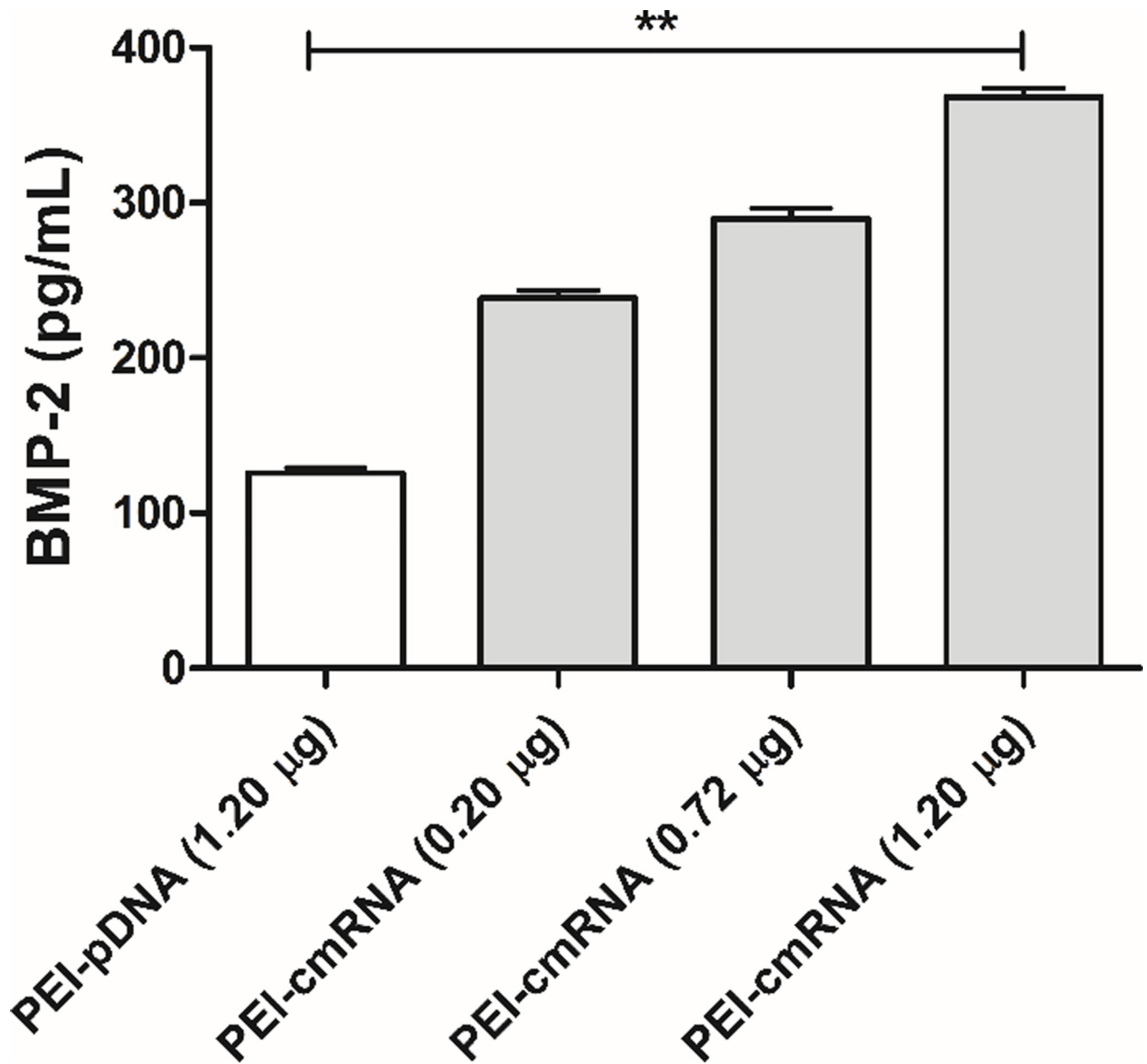


Fig. 4. ELISA assay demonstrating BMP-2 secretion from BMSCs at 48 h after transfection with PEI-cmRNA and PEI-pDNA polyplexes (prepared at a N/P ratio of 10 (1.2 µg cmRNA)). Significant differences between PEI-pDNA and PEI-cmRNA (1.20 µg) were assessed by Kruskal-Wallis nonparametric test followed by Dunns post-test (**p<0.01). Values are expressed as mean ± SD (n = 4).

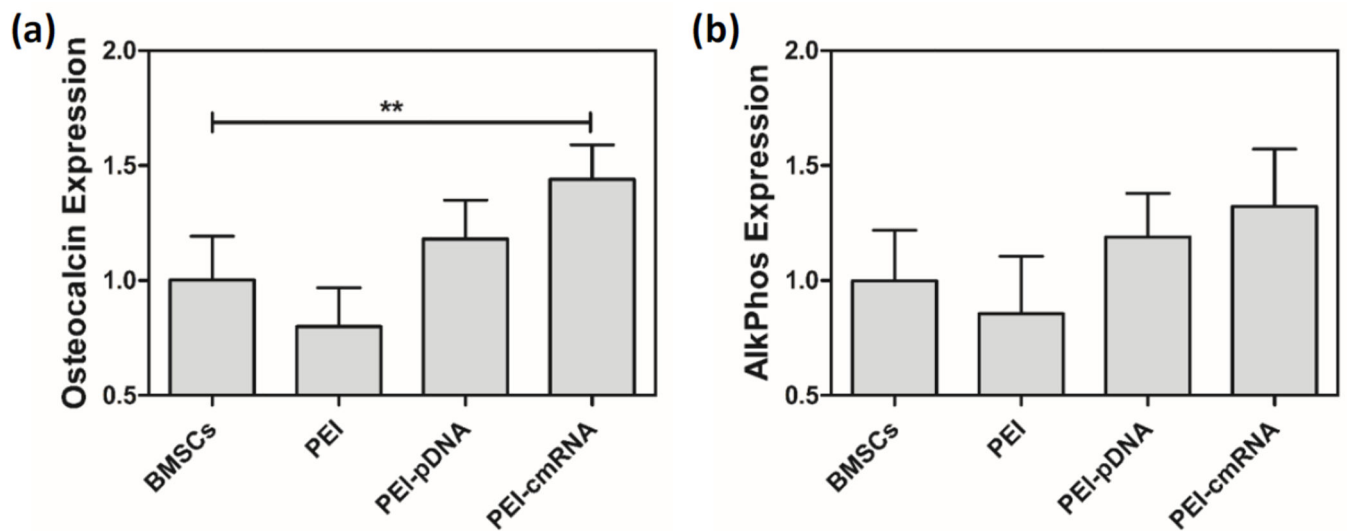


Fig. 5.

(a) *Osteocalcin* and (b) *alkaline phosphatase* mRNA levels in BMSCs were determined using real-time PCR analysis, 3 days after treatment with either PEI-cmRNA or PEI-pDNA polyplexes (prepared at a N:P ratio of 10 (1.2 μ g cmRNA)) (n = 4). Significant differences between the treatments and the untreated controls were assessed by one way ANOVA followed by Dunnett's multiple comparison post-test (**p < 0.01). Values are expressed as mean \pm SD.

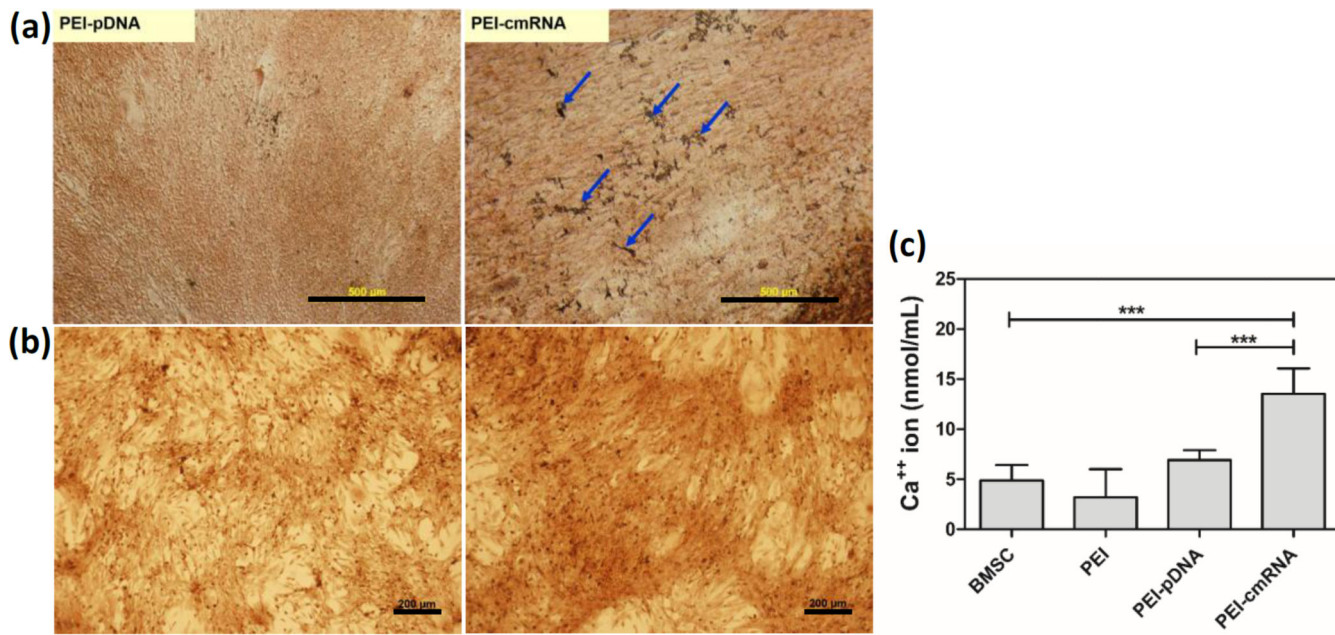


Fig. 6. (a) Von Kossa staining, arrows indicate black precipitations associated with calcium salt (scale bar, 500 μ m) (b) Alizarin red (scale bar, 200 μ m) staining (c) and atomic absorption performed to detect calcium mineralization produced by BMSCs 14 days after treatment with either PEI-cmRNA or PEI-pDNA polyplexes. Significant differences between the treatments and the untreated cells were assessed by one-way analysis of variance followed by Tukey's post-test (***) $p < 0.001$. Values are expressed as mean \pm SD (n=4).

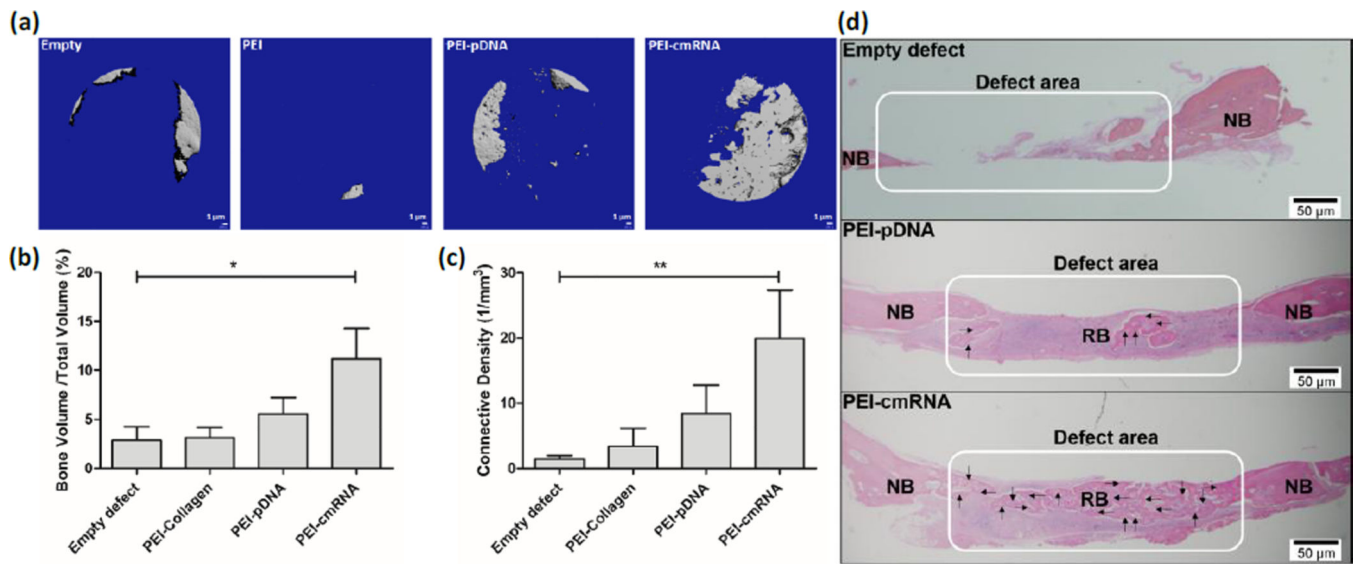


Fig. 7.

(a) Representative μ CT scans showing the level of regenerated bone tissue after 4 weeks in CBD treated with: empty defects, PEI-treated scaffolds, PEI-*pDNA* complex-loaded scaffolds, or PEI-cmRNA complex-loaded scaffolds (n=7). (b) Assessment of bone volume fraction and (c) connectivity density of regenerated bone after 4 weeks of implantation. Significant differences between PEI-cmRNA treatments and control group were assessed by Kruskal-Wallis nonparametric test followed by Dunns post-test (**p < 0.01, *p < 0.1). (Values are expressed as mean \pm SD). (d) Illustrative histology sections demonstrating the extent of new bone formation in the defects at 4 weeks due to various treatments. Note the complete bridging of new bone in the group treated with PEI-cmRNA-embedded scaffolds, and partial filling for the group treated with PEI-*pDNA*-embedded scaffolds. RB-regenerated bone and NB-native bone. Note the bridging of new bone in the PEI-cmRNA complex-loaded test group indicated by the arrows. Scale bar, 50 μ m.